JMEPEG (2015) 24:136–142
DOI: 10.1007/s11665-014-1299-7

1059-9495/$19.00

Effect of Pore Structure Regulation on the Properties of Porous TiNbZr Shape Memory Alloys for Biomedical Application

Ming Lai, Yan Gao, Bin Yuan, and Min Zhu

(Submitted May 17, 2014; in revised form October 5, 2014; published online November 13, 2014)

Recently, porous Ti-Nb-based shape memory alloys have been considered as promising implants for biomedical application, because of their non-toxic elements, low elastic modulus, and stable superelasticity. However, the inverse relationship between pore characteristics and superelasticity of porous SMAs will strongly affect their clinical application. Until now, there have been few works specifically focusing on the effect of pore structure on the mechanical properties and superelasticity of porous Ti-Nb-based SMAs. In this study, the pore structure, including porosity and pore size, of porous Ti-22Nb-6Zr alloys was successfully regulated by adjusting the amount and size of space-holder particles. XRD and SEM investigation showed that all these porous alloys had homogeneous composition. Compression tests indicated that porosity played an important role in the mechanical properties and superelasticity of these porous alloys. Those alloys with porosity in the range of 38.5%-49.7% exhibited mechanical properties approaching to cortical bones, with elastic modulus, compressive strength, and recoverable strain in the range of 7.2-11.4 GPa, 188-422 MPa, and 2.4%-2.6%, respectively. Under the same porosity, the alloys with larger pores exhibited lower elastic modulus, while the alloys with smaller pores presented higher compressive strength.

Keywords biomedical alloy, bone implant, modulus, pore structure, porous titanium alloy, recoverable strain

1. Introduction

Porous materials, which exhibit lower stiffness and better biological fixation than dense counterparts, have been presently applied in tissue engineering as potential bone substitutes. Comparing with porous ceramics and polymers, porous metals present higher strength that meets the mechanical requirements of implants under load-bearing conditions (Ref 1). Among these porous metals, porous NiTi shape memory alloys (SMAs) outstand for their unique shape memory effect and superelasticity, which can match the hysteretic behavior of bones and facilitate implant insertion, as well as good corrosion resistance that guarantee their functions in the body fluid (Ref 2). Even though porous NiTi SMAs have been widely reported as excellent candidates for biomedical applications, concerns still remain for the toxic and even carcinogenic element Ni which might be a potential threat to the health of patients (Ref 3). The ultimate solution to overcome the problem of Ni ion releasing is to develop Ni-free Ti-based SMAs with non-toxic and biocompatible elements (Ref 4).

Ming Lai, Yan Gao, Bin Yuan, and **Min Zhu,** School of Materials Science and Engineering, South China University of Technology, Guangzhou 510641, People's Republic of China. Contact e-mails: shudemingzai@gmail.com and meygao@scut.edu.cn.

Baker (Ref 5) had firstly found that cold-rolled Ti-35 wt.% Nb binary alloy possesses shape memory effect due to the reversible transformation from α''-phase to β-phase. Other researchers began to investigate the phase transformation behavior and superelasticity of Ti-Nb-based alloys recently because of their biomedical application potentials. Miyazaki et al. (Ref 6-9) systematically investigated Ti-Nb and Ti-Nb-X (where X = Ta, Zr, O) alloys and found that the martensitic transformation start temperature (M_s) decreased with increasing Nb and Zr content. The M_s of Ti-22Nb-(2,4,6)Zr at.% were evaluated to be 358, 283, and 200 K, respectively. Even though the M_s of Ti-22Nb-6Zr alloy (200 K) was much lower than room temperature, a maximum recoverable strain as high as 4.3% was observed in these alloys, which is sufficient for most biomedical applications, especially in bone replacement (Ref 3). Although the results of Ti-22Nb-(2,4,6)Zr were favorable, all these Ti-Nb-Zr SMAs were dense materials, with elastic modulus much higher than natural bones (Ref 10). Thus, it is necessary to develop porous Ti-Nb-Zr SMAs with lower elastic modulus to match that of human bones so as to prevent stress shielding effect, which may lead to bone resorption near the implants (Ref 11).

There have been only a few reports about porous TiNbZr alloys in the very recent years (Ref 12-15). Wang et al. (Ref 15) fabricated porous Ti-10Nb-10Zr wt.% alloy scaffolds with porosities in the range of 42%-74% using conventional sintering (CS) method. Among these porous TiNbZr alloys, the sample with 59% porosity exhibits an elastic modulus as low as 5.6 GPa while maintaining its plateau stress at 137 MPa. But all these alloys did not exhibit shape memory effect or superelasticity. Brailovski et al. (Ref 12, 13) fabricated porous Ti-(18-20)Nb-(5,6)Zr (at.%) alloys using a polymer-based

foaming process, with porosity, elastic modulus, and compression strength in the range of 45-66%, 3.7-7.5 GPa, and 70-225 MPa, respectively. These porous alloys, however, exhibited only limited superelastisity of around 2.0%-2.5%. Ma et al. (Ref 14) sintered porous Ti-22Nb-6Zr (at.%) alloys by hot isostatic pressing method, with nearly spherical pores and complete superelasticity of 3% in solution-treated alloys, but the porosities of these samples are around 12%, which could not meet the requirement of porosity (30%-90%) for biomedical implants. The inverse relationship between pore structure (such as porosity, pore size) and superelasticity of porous Ti-Nb-Zr SMAs will strongly affect their clinical application, so it is necessary to improve the match between high porosity or pore size and low superelasticity by pore structure regulation of porous Ti-Nb-Zr SMAs.

In this study, the pore structure, such as porosity and pore size, of porous Ti-22Nb-6Zr (at.%) alloys was regulated by adjusting the amount and size of space-holder particles. Then, the porous Ti-22Nb-6Zr alloys with different structures were successfully fabricated using vacuum sintering. The effect of pore structure regulation on mechanical properties and superelasticity of these porous Ti-22Nb-6Zr alloys were systematically analyzed, which might provide some advices for future design of porous alloys for biomedical application, especially as implants in bone replacement.

2. Materials and Methods

2.1 Specimen Preparation

The elemental metal powders of Ti (purity > 99.5%, particle size < 75 μm), Nb (purity > 99%, particle size < 75 μm), and Zr (purity > 99%, particle size < 75 μm) were mixed at a nominal composition of Ti-22Nb-6Zr (at.%) and blended for 4 h in a planetary ball milling system with stainless steel containers and balls, with a weight ratio of ball to powder of 2:1 and rotation rate of 200 rpm. The space-holder material used in this study is ammonium hydrogen carbonate (NH_4HCO_3), which was sifted to different sizes and then blended with the pre-mixed Ti-22Nb-6Zr powders for 0.5 h. The mixed powders (Ti-22Nb-6Zr and NH_4HCO_3) were then cold pressed into some cylindrical green compacts using a hydraulic press machine. The compacts from the mixed powders were sintered in a tube furnace in two steps with a vacuum of 10^{-2}-10^{-3} Pa. The first step was to hold the temperature at 200 °C for 1 h so that the space-holder particles can be burnt out. Then, the green compacts were heated up to 1400 °C and held for 10 h under argon atmosphere. By adding 0, 7.5, 15, 30, 45, and 60 wt.% sifted NH_4HCO_3 particles to the powder mixture, porous Ti-22Nb-6Zr alloys with porosities of 6.7%, 16.4%, 26.9%, 38.5%, 49.7%, and 57.6% were fabricated. As for the alloys with different pore sizes, porous alloys with porosities of 38.4%, 38.5%, and 39.3% were fabricated by adding the same amount of NH_4HCO_3 particles (30 wt.%) with sizes of 75-150, 200-250, and 300-355 μm, respectively.

2.2 Characterization of Specimen

The phase constituents of Ti-22Nb-6Zr alloys were analyzed by x-ray diffractometer (XRD, Philips x'pert MPD with Cu-Kα radiation). A scanning electron microscopy (SEM, LEO 1530 VP FE-SEM) with energy dispersive x-ray spectroscope (EDS) accessory was used to determine the microstructure and composition. The impulse inert gas fusion method performed on a LECO TC-600 Oxygen-Azote determinator was used to measure oxygen content (wt.%) in the alloys, which was then converted into atom percent (at.%) by calculating together with EDS results. The phase transformation temperatures of porous Ti-22Nb-6Zr alloys were measured by differential scanning calorimetry (DSC) with heating and cooling rate of 10 °C/min, using a Netzsch DSC-204 calorimeter. The density of specimens was measured by the Archimedes' principle. A Leica DMI5000M optical microscope was used to characterize the pore structure. The cylindrical samples with a diameter of 3 mm and length of 6 mm were used for compression test. The size and dimension of the samples were designed with a length/diameter ratio of 2.0 according to ASTM: E9-09. Compression tests were performed on an Instron 5567 test system at an initial strain rate of 5.56×10^{-4} s^{-1}. For each condition, three samples were tested, and results are presented in the form of mean value with standard deviation. All the tests were performed at room temperature.

3. Results and Discussions

3.1 Pore Characteristics

Figure 1 shows the optical micrographs of porous Ti-22Nb-6Zr alloys with the porosities ranging from 6.7% to 57.6%. The porous alloys were fabricated using NH_4HCO_3 of 200-250 μm as space-holder particles, except for the alloy with porosity of 6.7% (Fig. 1a), which was prepared without any space-holder but still contained pores in the range 1-20 μm. The porosities of these porous alloys can be precisely controlled by adding specified amount of space-holder particles in green samples before sintering. As presented in Fig. 1(b)-(f), the pores were all in the shape of irregular polygon as the space-holder, and the pore sizes were mainly in the range of 200-250 μm, which was also consistent with the size of space-holder particles. Moreover, the pores in the samples with porosity of 6.7%-26.9% tend to be separate with each other, resulting in a low interconnectivity of the alloys. While with increasing porosity (38.5% or even higher), the pores incline to connect with each other and the interconnectivity is higher with higher porosity, which is beneficial for porous materials due to the better cell growth and body fluid circulation in these connected pores (Ref 16).

The optical micrographs of porous Ti-22Nb-6Zr alloys with the same porosity and different pore sizes were presented in Fig. 2. These alloys were fabricated using space-holder particles of different sizes, and their porosities were controlled to be almost the same (around 38%). It is obvious that the pore size of porous alloys can be regulated by adjusting the sizes of space-holder particles. The diameters of pores in Fig. 2(a-c) are in the range of 75-150, 200-250, and 300-355 μm, respectively. In addition, it can be seen that with larger size, the probability of the formation of inter-connective pores is higher (Fig. 2c), resulting in a higher interconnectivity in the porous alloys, which is helpful for porous implants as mentioned above.

The chemical compositions of all these porous alloys were close to the nominal compositions of Ti-22Nb-6Zr as shown in Table 1. The difference between the actual chemical compositions and nominal compositions of the alloys might be the

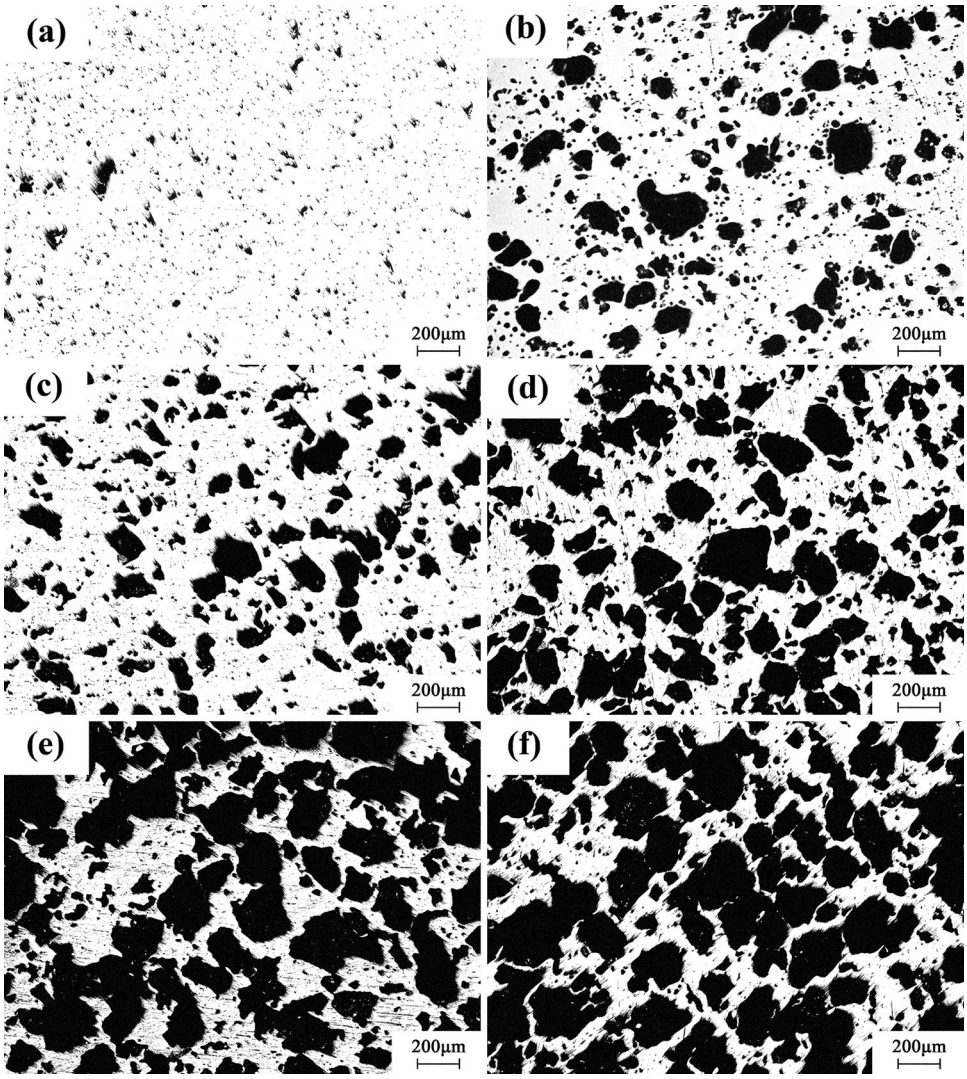

Fig. 1 Optical micrographs of porous Ti-22Nb-6Zr alloys with different porosities: (a) 6.7% (b) 16.4% (c) 26.9%, (d) 38.5% (e) 49.7 (f) 57.6%

result of the inevitable inhomogeneity in the alloy compositions (Ref 2). The minimal difference of chemical constitutions among all these porous alloys would guarantee that the varieties of mechanical properties investigated later were mainly caused by different pore structures.

3.2 Phase Constituents and Transformation Behavior

The phase constituents of porous Ti-22Nb-6Zr alloys with different porosities and sizes were analyzed by XRD and presented in Fig. 3. All these porous alloys consist of pure β-phase at room temperature, indicating that the pore structure has almost no effect on phase constituents. These porous Ti-22Nb-6Zr alloys with β-phase structure will have advantage of lower elastic modulus over α-Ti or (α + β)-Ti alloys to better match natural bones (Ref 17).

The phase transformation behavior of porous Ti-22Nb-6Zr alloys was measured by DSC between −70 and 400 °C and is shown in Fig. 4. No phase transformation peaks were detected in the range of −70 to 400 °C, and therefore it can be deduced that the martensitic transformation start temperature (M_s) should be lower than −70 °C, since all these porous alloys consist of pure β-phase at room temperature (Fig. 3). The M_s of dense Ti-22Nb-6Zr alloy is reported to be around 200-220 K (−73 to −53 °C) (Ref 8). As for the porous samples in this work, their lower M_s might be caused by solid-solution of oxygen during the sintering process, since oxygen would greatly decrease the martensitic transformation temperature of Ti-Nb-based alloys (Ref 7, 18).

3.3 Mechanical Properties

The compressive rupture curves and cyclic stress-strain curves of porous Ti-22Nb-6Zr alloys with porosity ranging from 6.7% to 57.6% are shown in Fig. 5. The calculated elastic moduli, compressive stresses, and recoverable strain are given in Table 2. As for the Ti-22Nb-6Zr alloy with 6.7% porosity, the elastic modulus (29.8 GPa) is much lower than (α + β) type Ti-10Nb-10Zr alloy (68 GPa, 4% porosity) (Ref 15), and the compressive stress is as high as 1615 MPa accompanied with a favorable recoverable strain of 4.1%. The elastic modulus, compressive stress, and recoverable strain decreased with increasing porosity. In the porous Ti-22Nb-6Zr alloy with porosity of 57.6%, the elastic modulus can be as low as

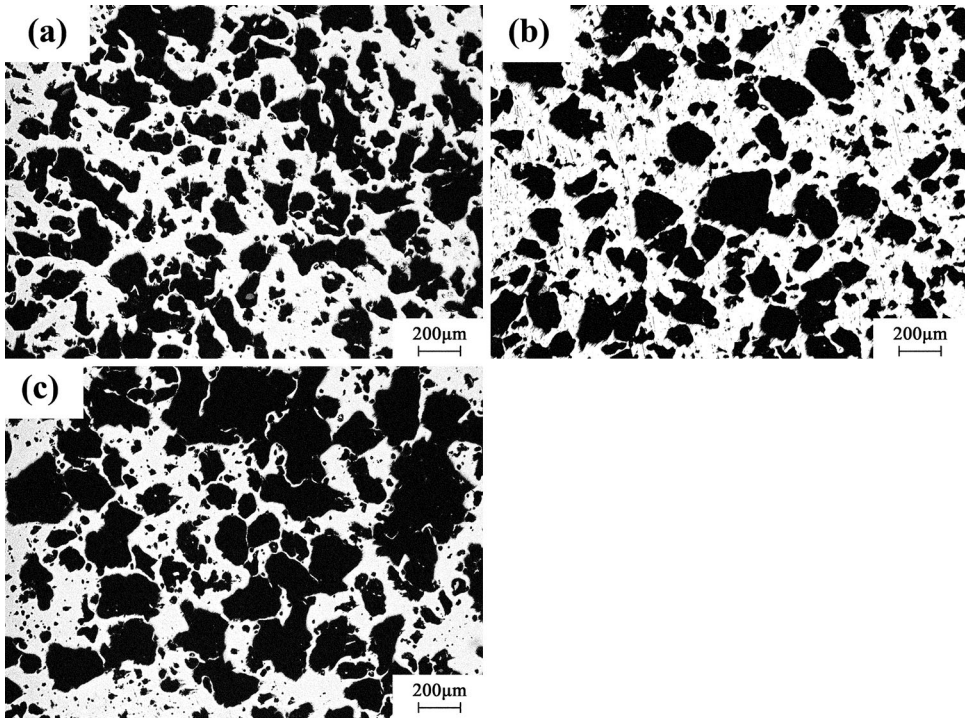

Fig. 2 Optical micrographs of porous Ti-22Nb-6Zr alloys with different pore sizes under similar porosity of 38.5%: (a) 75-150 μm (b) 200-250 μm (c) 300-355 μm

Table 1 EDS results of porous Ti-22Nb-6Zr alloys with different porosities

Porosity, %	Ti, at.%	Nb, at.%	Zr, at.%
6.7	73.3	20.7	6.0
16.4	72.0	21.5	6.5
26.9	74.0	20.1	5.9
38.5	74.0	19.8	6.2
49.7	72.3	21.4	6.3
57.6	73.8	20.3	5.9

4.3 GPa, which is close to that of natural trabecular bone (0.4-3.6 GPa) (Ref 19). In addition, the porous Ti-22Nb-6Zr alloys with porosity ranging from 38.5% to 49.7% exhibit mechanical properties approaching to cortical bones (20-30 GPa) (Ref 20) with elastic modulus, compressive strength, and recoverable strain in the range of 7.2-11.4 GPa, 188-422 MPa, and 2.4%-2.6%, respectively.

Under the similar porosity ($38.5 \pm 1\%$), the pore size seems to have little effect on recoverable strain as shown in Fig. 6 and Table 3. The alloy with largest pore size exhibits relatively low elastic modulus (9.7 GPa) while it maintains a compressive strength of 372 MPa.

Porosity is an important structural factor that dramatically influences the mechanical properties of porous alloys, just as proposed by Gibson and Ashby (Ref 21) that relative density is the most significant structural factor affecting the mechanical behavior of foams. In this work, the elastic modulus, compressive strength, and recoverable strain of porous Ti-22Nb-6Zr alloys all decreased with increasing porosity (Fig. 7). According to Gibson-Ashby model (Ref 21), the structure of the porous material can be simplified to an open-cell porous material, which consists of periodically arranged units. Under compression tests, the deformation of the porous metal might be assumed as the bending of unit struts. With higher porosity, the struts of the unit are thinner, leading to a lower compressive stress that the porous alloys can bear. Ergo, the compressive strength decreases with the increase of porosity. Meanwhile, it is worthy to notice that other structural characteristics such as pore size might also affect their mechanical behavior, which is also shown in Fig. 7.

The pore sizes of porous Ti-22Nb-6Zr alloys were successfully regulated by adding sifted space-holder particles with three different sizes: $75 \sim 150$ μm (triangle points in Fig. 7), 200-250 μm (square points in Fig. 7), and 300-355 μm (round points in Fig. 7). It can be seen that under the same porosity (38%), the alloys with smaller pores (75-150 μm) present higher compressive strength, which might be ascribed to their relatively homogeneous pore distribution and thick struts (Fig. 2a). In contrast, the 300-355 μm samples possess much larger pores which incline to be inter-connective, resulting in much thinner struts formed in the alloys (Fig. 2c). Under compressive condition, these thin struts are easily broken, causing the fracture of the porous sample. Therefore, the 75-150 μm sample, the struts of which are relatively thick, has the highest compressive strength. In the meantime, it should be noted that even though the $300 \sim 355$ μm samples exhibit relatively lower compressive strength (372 MPa), they can still meet the requirement of bone implants (200 MPa) (Ref 20). The benefit of regulating pore sizes is obvious. If the mechanical parameters of a porous metal with a desired porosity could not meet biomedical requirement, the pore size can be adjusted to improve its mechanical properties to some extent. With larger pores, the porous alloys of the same

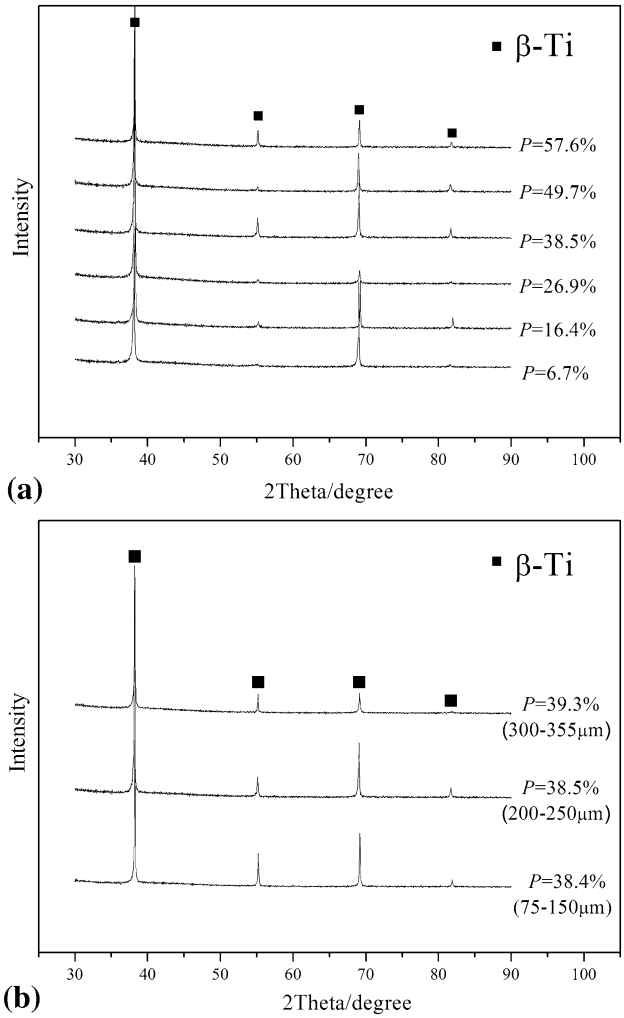

Fig. 3 XRD patterns of porous Ti-22Nb-6Zr alloys with (a) different porosities and (b) different pore sizes

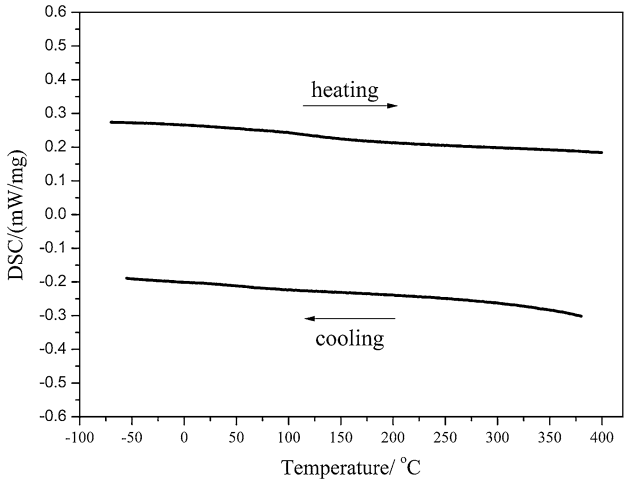

Fig. 4 DSC curves of porous Ti-22Nb-6Zr alloy with porosity of 6.7%

porosity possess even lower elastic modulus, which is closer to that of natural bones, thus to prevent stress shielding effect (Ref 22, 23).

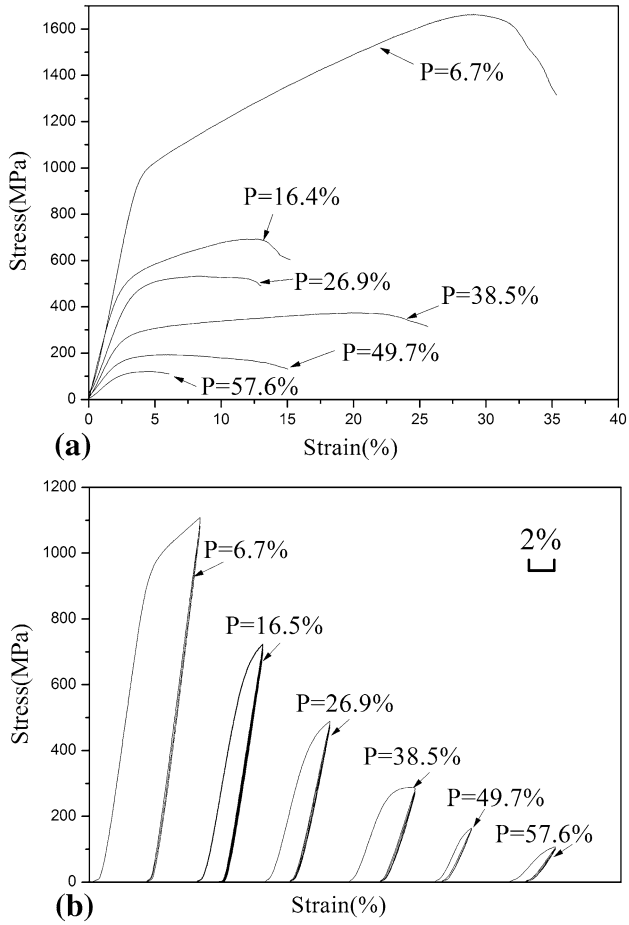

Fig. 5 Compressive rupture curves (a) and cyclic stress-strain curves (b) of porous Ti-22Nb-6Zr alloys with different porosities

Moreover, the recoverable strains seem to have very limited change by adjusting pore sizes. For all these samples with porosity of around 38%, their recoverable strains vary in the range of 2.6%-2.8%, which are slightly lower than the requirement (3%) of bone implants. Unlike porous NiTi alloys, whose superelasticity remained over 5% with porosity of 43% (Ref 24), porous Ti-Nb-Zr alloys exhibit a much lower recoverable strain. In this case, the recoverable strains of all these porous Ti-Nb-Zr alloys are considered to be mainly contributed by the elasticity of their pore structures other than their superelasticity, just as natural bones exhibit a recoverable strain over 2% after the applied stress is released (Ref 25).

Our deeper research (Ref 26) has revealed that porous Ti-22Nb-6Zr alloys fabricated via vacuum sintering exhibited a recoverable strain of around 6% at −85 °C, indicating that the alloys own very good SME and superelasticity intrinsically but may not show these characters at room temperature due to their very low martensitic transformation start temperature (M_s). Our further works will focus on adjusting the M_s of these porous alloys to around room temperature by largely decreasing the Nb and Zr contents, so as to improve their superelasticity at room temperature. Moreover, we will also optimize the sintering process of porous Ti-Nb-Zr alloys by adding reductant in the mixed powders in order to reduce the oxygen content induced during sintering, consequently minimizing the effect of oxygen on the phase transformation behavior of Ti-Nb-Zr SMAs.

Table 2 Mechanical parameter obtained from compression tests

Porosity, %	Elastic modulus, GPa	Compressive strength, MPa	Recoverable strain, %
6.7	29.8 (1.0)[a]	1615 (41)	4.1 (0.1)
16.4	23.3 (1.7)	791 (90)	3.2 (0.2)
26.9	15.1 (1.0)	557 (33)	2.9 (0.2)
38.5	11.4 (0.4)	422 (48)	2.6 (0.1)
49.7	7.2 (0.6)	188 (6)	2.4 (0.1)
57.6	4.3 (0.8)	139 (17)	2.3 (0.1)

[a]Standard deviations are shown in parentheses

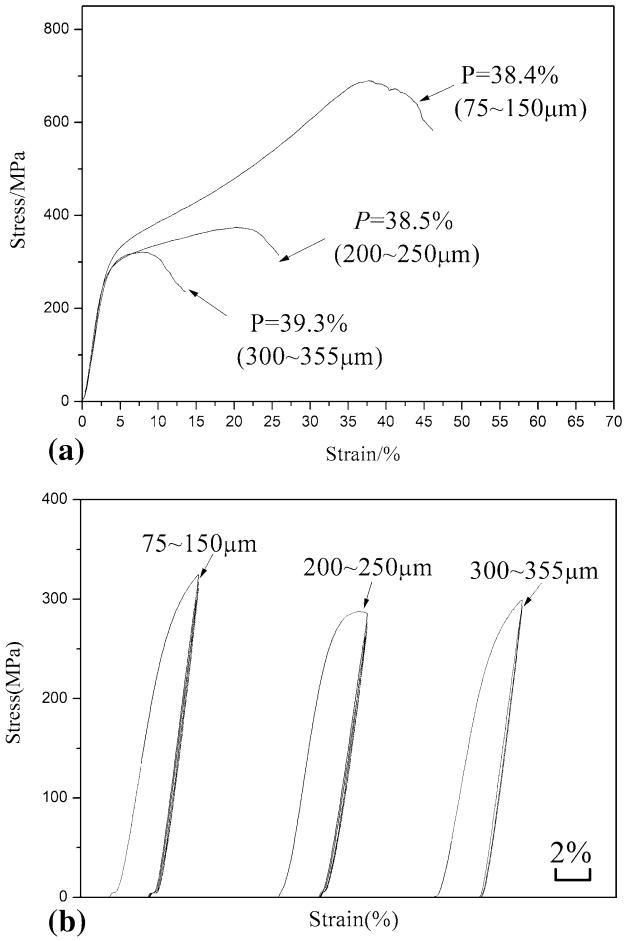

Fig. 6 Compressive rupture curves (a) and cyclic compressive stress-strain curves (b) of porous Ti-22Nb-6Zr alloys with different pore sizes

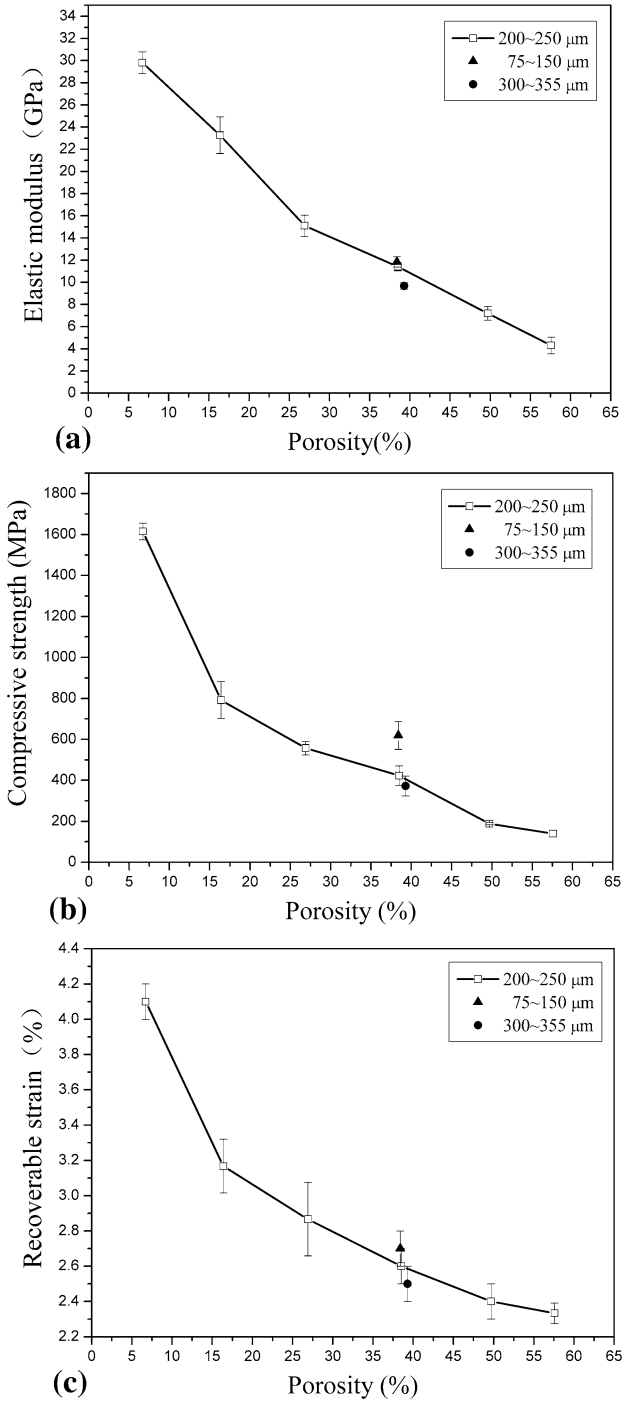

Fig. 7 Elastic modulus (a), compressive strength (b), and recoverable strain (c) of porous Ti-22Nb-6Zr alloys with different porosities and pore sizes

Table 3 Mechanical parameters of porous Ti-22Nb-6Zr alloys with different pore sizes

Porosity, %	Pore size, μm	Elastic modulus, GPa	Compressive strength, MPa	Recoverable strain, %
38.4	75-150	11.8 (0.5)[a]	619 (68)	2.7 (0.1)
38.5	200-250	11.4 (0.4)	422 (48)	2.6 (0.1)
39.3	300-355	9.7 (0.3)	372 (49)	2.5 (0.1)

[a]Standard deviations are shown in parentheses

4. Conclusions

The pore structures including porosities and pore sizes of porous Ti-22Nb-6Zr alloys with homogeneous constitution were successfully regulated by conventional sintering methods. Even though the very low M_s temperature of all these porous Ti-22Nb-6Zr alloys results in the limited superelasticity exhibited at room temperature, the important effect of pore structures on the mechanical properties and superelasticity could still be observed. Appropriate porosities for porous Ti-22Nb-6Zr alloys are found to be between 38.5%-49.7%, with mechanical properties approaching to cortical bones (Elastic modulus, compressive strength, and recoverable strain of the alloys are in the range of 7.2-11.4 GPa, 188-422 MPa, and 2.4%-2.6%, respectively). Under the same porosity, the alloys with larger pores exhibit lower elastic modulus, while the alloys with smaller pores present higher compressive strength.

Acknowledgments

The authors acknowledge the supports from Guangdong Provincial Science and Technology Projects (2012B010200020), New Century Excellent Talents in University (NCET-12-0201), and Fundamental Research Funds for the Central Universities (2014ZG0026) and Guangdong Natural Science Funds (S2013010012487).

References

1. K. Rezwan, Q.Z. Chen, J.J. Blaker, and A.R. Boccaccini, Biodegradable and Bioactive Porous Polymer/Inorganic Composite Scaffolds for Bone Tissue Engineering, *Biomaterials*, 2006, **27**(18), p 3413–3431
2. M.H. Elahinia, M. Hashemi, M. Tabesh, and S.B. Bhaduri, Manufacturing and Processing of NiTi Implants: A Review, *Prog. Mater. Sci.*, 2012, **57**, p 911–946
3. A. Biesiekierski, J. Wang, M. Gepreel, and C.E. Wen, A New Look at Biomedical Ti-Based Shape Memory Alloys, *Acta Biomater.*, 2012, **8**(5), p 1661–1669
4. S. Miyazaki, H.Y. Kim, and H. Hosoda, Development and Characterization of Ni-Free Ti-Base Shape Memory and Superelastic Alloys, *Mater. Sci. Eng. A.*, 2006, **438-440**, p 18–24
5. C. Baker, The Shape-Memory Effect in a Titanium-35 wt.% Niobium Alloy, *Met. Sci. J.*, 1971, **5**, p 92–100
6. H.Y. Kim, Y. Ikehara, J.I. Kim, H. Hosoda, and S. Miyazaki, Martensitic Transformation, Shape Memory Effect and Superelasticity of Ti-Nb Binary Alloys, *Acta Mater.*, 2006, **54**(9), p 2419–2429
7. J.I. Kim, H.Y. Kim, H. Hosoda, and S. Miyazaki, Shape Memory Behavior of Ti-22Nb-(0.5-2.0)O(at.%) Biomedical Alloys, *Mater. Trans.*, 2005, **46**(4), p 852–857
8. J.I. Kim, H.Y. Kim, T. Inamura, H. Hosoda, and S. Miyazaki, Shape Memory Characteristics of Ti-22Nb-(2-8)Zr(at.%) Biomedical Alloys, *Mater. Sci. Eng. A*, 2005, **403**(1-2), p 334–339
9. Y. Fukui, T. Inamura, H. Hosoda, K. Wakashima, and S. Miyazaki, Mechanical Properties of a Ti-Nb-Al Shape Memory Alloy, *Mater. Trans.*, 2004, **45**(4), p 1077–1082
10. J.Y. Rho, T.Y. Tsui, and G.M. Pharr, Elastic Properties of Human Cortical and Trabecular Lamellar Bone Measured by Nanoindentation, *Biomaterials*, 1997, **18**(20), p 1325–1330
11. G. Ryan, A. Pandit, and D.P. Apatsidis, Fabrication Methods of Porous Metals for Use in Orthopaedic Applications, *Biomaterials*, 2006, **27**(8), p 2651–2670
12. V. Brailovski, S. Prokoshkin, M. Gauthier, K. Inaekyan, and S. Dubinskiy, Mechanical Properties of Porous Metastable Beta Ti-Nb-Zr Alloys for Biomedical Applications, *J. Alloy. Compd.*, 2013, **577**, p S413–S417
13. V. Brailovski, S. Prokoshkin, M. Gauthier, K. Inaekyan, S. Dubinskiy, M. Petrzhik, and M. Filonov, Bulk and Porous Metastable Beta Ti-Nb-Zr(Ta) Alloys for Biomedical Applications, *Mater. Sci. Eng. C.*, 2011, **31**(3), p 643–657
14. L.W. Ma, C.Y. Chung, Y.X. Tong, and Y.F. Zheng, Properties of Porous TiNbZr Shape Memory Alloy Fabricated by Mechanical Alloying and Hot Isostatic Pressing, *J. Mater. Eng. Perform.*, 2011, **20**(4-5), p 783–786
15. X.J. Wang, Y.C. Li, J.Y. Xiong, P.D. Hodgson, and C.E. Wen, Porous TiNbZr Alloy Scaffolds for Biomedical Applications, *Acta Biomater.*, 2009, **5**(9), p 3616–3624
16. J.P. Li, J.R. Wijn, C.A. Van Blitterswijk, and K. Groot, Porous Ti_6Al_4V Scaffold Directly Fabricating by Rapid Prototyping: Preparation and In Vitro Experiment, *Biomaterials*, 2006, **27**(8), p 1223–1235
17. M. Niinomi, Recent Research and Development in Titanium Alloys for Biomedical Applications and healthcare goods, *Sci. Technol. Adv. Mater.*, 2003, **4**(5), p 445–454
18. A. Terayama, N. Fuyama, Y. Yamashita, I. Ishizaki, and H. Kyogoku, Fabrication of Ti-Nb Alloys by Powder Metallurgy Process and Their Shape Memory Characteristics, *J. Alloy. Compd.*, 2013, **577**, p S408–S412
19. S.D. Ryan and J.L. Williams, Tensile Testing of Rodlike Trabeculae Excised from Bovine Femoral Bone, *J. Biomech.*, 1989, **22**(4), p 351–355
20. X.J. Wang, Y.C. Li, P.D. Hodgson, and C.E. Wen, Nano- and Macro-Scale Characterisation of the Mechanical Properties of Bovine Bone, *Mater. Forum*, 2007, **31**, p 156–159
21. L.J. Gibson and M.F. Ashby, *Cellular Solids: Structure and Properties*, 2nd ed., Cambridge University Press, Cambridge, 1999, p 183–197
22. D. Lin, C. Chuang, J. Chern Lin, J. Lee, C. Ju, and H. Yin, Bone Formation at the Surface of Low Modulus Ti-7.5Mo Implants in Rabbit Femur, *Biomaterials*, 2007, **28**(16), p 2582–2589
23. E.B. Taddei, V.A.R. Henriques, C.R.M. Silva, and C.A.A. Cairo, Production of New Titanium Alloy for Orthopedic Implants, *Mater. Sci. Eng. C*, 2004, **24**(5), p 683–687
24. T. Aydogmus and S. Bor, Superelasticity and Compression Behavior of Porous TiNi Alloys Produced Using Mg Spacers, *J. Mech. Behav. Biomed.*, 2012, **15**, p 59–69
25. S.A. Shabalovskaya, On the Nature of the Biocompatibility and on Medical Applications of NiTi Shape Memory and Superelastic Alloys, *Bio-Med. Mater. Eng.*, 1996, **6**(4), p 267–289
26. M. Lai, Y. Gao, B. Yuan, and M. Zhu, Indirect Determination of Martensitic Transformation Temperature of Sintered Nickel-Free Ti-22Nb-6Zr Alloy by Low Temperature Compression Test, *Mater. Des.*, 2014, **60**, p 193–197